

Article

Pairing Superfluid–Insulator Transition Induced by Atom–Molecule Conversion in Bosonic Mixtures in Optical Lattice

Haiming Deng ¹, Zhi Tan ², Chao Kong ¹, Fuqiu Ye ³ and Honghua Zhong ^{2,*}

¹ School of Physics and Electronic-Electrical Engineering, Xiangnan University, Chenzhou 423000, China; woshidenghaiming@126.com (H.D.); superkong@xnu.edu.cn (C.K.)

² Institute of Mathematics and Physics, Central South University of Forestry and Technology, Changsha 410004, China; veigar_007@163.com

³ Department of Physics, Jishou University, Jishou 416000, China; phyfq@jsu.edu.cn

* Correspondence: hhzhong115@163.com

Abstract: Motivated by the recent experiment on bosonic mixtures of atoms and molecules, we investigate pairing superfluid–insulator (SI) transition for bosonic mixtures of atoms and molecules in a one-dimensional optical lattice, which is described by an extended Bose–Hubbard model with atom–molecule conservation (AMC). It is found that AMC can induce an extra pair–superfluid phase though the system does not demonstrate pair-hopping. In particular, the system may undergo several pairing SI or insulator–superfluid transitions as the detuning from the Feshbach resonance is varied from negative to positive, and the larger positive detuning can bifurcate the pair–superfluid phases into mixed superfluid phases consisting of single-atomic and pair-atomic superfluid. The calculation of the second-order Rényi entropy reveals that the discontinuity in its first-order derivative corresponds to the phase boundary of the pairing SI transition. This means that the residual entanglement in our mean-field treatment can be used to efficiently capture the signature of the pairing SI transition induced by AMC.

Keywords: bosonic mixtures; optical lattice; pair–superfluid



Citation: Deng, H.; Tan, Z.; Kong, C.; Ye, F.; Zhong, H. Pairing Superfluid–Insulator Transition Induced by Atom–Molecule Conversion in Bosonic Mixtures in Optical Lattice. *Symmetry* **2023**, *15*, 1715. <https://doi.org/10.3390/sym15091715>

Academic Editor: Manuel Gadella

Received: 19 July 2023

Revised: 16 August 2023

Accepted: 23 August 2023

Published: 7 September 2023



Copyright: © 2023 by the authors. Licensee MDPI, Basel, Switzerland. This article is an open access article distributed under the terms and conditions of the Creative Commons Attribution (CC BY) license (<https://creativecommons.org/licenses/by/4.0/>).

1. Introduction

Quantum gas mixtures in optical lattices provide an ideal testing ground to investigate interaction-induced effects in condensed matter [1–3], such as the bosonic superfluid (SF) to Mott-insulator (MI) transition in the presence of fermionic atoms [4–8] or molecules [9,10]. Recently, a coherent conversion between Cs atomic Bose–Einstein condensate (BEC) and the condensate of molecules Cs₂ was experimentally demonstrated by changing a magnetic field in time that pushed the ultracold atoms across the Feshbach resonance [11]. The coherent coupling between atoms and molecules has been utilized to observe atom–molecule Rabi oscillations [12,13], dynamics of matter waves [14], and predict quantum phase transition between mixed atom–molecule and purely molecular condensates [9,15–23]. The fundamental characteristic of the atom–molecule coupling is its nonlinear nature; only pairs of atoms can be converted to molecules, which can lead to a strong density dependence of atom–molecule conversion (AMC) [24–26]. It is important that this aspect can induce novel SF phase with both an atomic and a molecular condensate [17–19], super-Mott phase [20,21], Feshbach insulator [22], and MI to SF transition [23,27–29].

Pair-SF phase has been observed in Bose–Hubbard models with explicit correlated or pair-hopping processes [30–35], where a lesser known mechanism for pairing is correlated to hopping that could lead to the formation of bound atom pairs. Motivated by the possibility of stabilizing pairing phases of bosons in cold atomic gases, the pairing problem of binary Bose mixtures in optical lattices has also been investigated [36–40], where strong attractive mutual interaction can produce a dissipationless drag, and then the bosons are tightly paired and transport is only via pair-SF. The phenomenon of bosonic pairing

has recently been investigated in one-dimensional optical lattices containing mixtures of bosonic atoms and molecules using the large-scale density matrix renormalization group method [18]. The Feshbach resonant pairing interaction has been utilized to investigate the nature of the SF phase transition between the molecular condensate and the coupled atomic–molecular condensate. In this study, the von Neumann entropy was considered as indicative of the quantum phase transition between these states. However, the effect of AMC on pairing superfluid–insulator (SI) transition in the process of coherent conversion between atomic BEC and the condensate of molecules is still unclear. In particular, knowledge on how to efficiently and rapidly extract the signature of pairing SI transition is also lacking.

The entanglement entropy (EE) has been regarded as a typical signature of quantum phase transition in various many-body quantum systems [41–55]. Recently, the second-order Rényi EE in a bosonic SI transition has also been experimentally measured for ultracold bosonic atoms in optical lattices [56]. Up to now, the density matrix renormalization group method has been devoted to calculating the first-order EE (the von Neumann entropy) in extended Bose–Hubbard systems with AMC [18]. While the calculation of von Neumann entropy for infinite systems can effectively identify quantum phase transitions, it requires substantial computational resources and a significant amount of time. The mean-field (MF) approach, which is computationally efficient and time-saving, has been successfully employed to predict the occurrence of numerous quantum phase transitions in Bose–Hubbard systems. Can the MF approach capture the signature of EE in the emerged pairing SI transition induced by AMC?

In this work, we investigate pairing SI transition and its MF signature of EE for bosonic mixtures of atoms and molecules in a one-dimensional optical lattice by using the MF approach. In addition to the SF and integer MI phases, it is found that AMC can induce an extra pair-SF phase, though the system does not possess a pair-hopping. Depending on the strength of the AMC and the single atomic hopping, the ground state can be an MI, a mixed SF phase with both single-atomic and pair-atomic, or a pair-SF phase. Especially, the ground-state can undergo several pairing SI or insulator-superfluid transitions as the detuning is varied from negative to positive, and the larger positive detuning can bifurcate the pair-SF phases into mixed SF phases consisting of single-atomic and pair-atomic SF. Through the analysis of the second-order Rényi EE, we observe that the discontinuity in its first-order derivative aligns with the critical point of the pairing SI phase transition. This indicates that our MF approach effectively captures the EE signature during the AMC-induced pairing SI phase transition.

The structure of this article is as following. In Section 2, we introduce the Hamiltonian for our physical system and our MF treatment. In Section 3, we explore the effects of the AMC and detuning on ground-state phase diagram. We show the AMC-induced pair-SF and its robustness against atomic hopping in Section 3.1, and discuss the effect of detuning on ground-state phase diagrams in Section 3.1. In Section 4, we show the relation between the second-order Rényi EE and pairing SI phase transition. Finally, we give a conclusion in Section 5.

2. Model

The system under consideration is bosonic mixtures of atoms and molecules in a one-dimensional optical lattice with AMC, which allows two atoms to turn into a molecule and vice versa. If the optical potential is sufficiently deep, and AMC is sufficiently smaller than band-gap, the system can be described by a single-band Bose–Hubbard model with an atom–molecule coherent mixture [20,22,23]:

$$\begin{aligned}
\hat{H}_{AMC} = & - \sum_{\langle i,j \rangle} \left(J_a \hat{a}_i^\dagger \hat{a}_j + J_m \hat{m}_i^\dagger \hat{m}_j + H.c. \right) \\
& + \sum_i \left[\frac{U_a}{2} \hat{n}_i^a (\hat{n}_i^a - 1) + \frac{U_m}{2} \hat{n}_i^m (\hat{n}_i^m - 1) \right] \\
& + \sum_i [U_{am} \hat{n}_i^a \hat{n}_i^m - \mu (\hat{n}_i^a + 2\hat{n}_i^m)] \\
& - g \sum_i (\hat{m}_i^\dagger \hat{a}_i \hat{a}_i + \hat{a}_i^\dagger \hat{a}_i^\dagger \hat{m}_i) \\
& + \Delta \sum_i \hat{n}_i^m.
\end{aligned} \tag{1}$$

Here, $\langle i, j \rangle$ indicates the summation comprising all nearest-neighboring sites in the chain, and the parameters J_a and J_m are atomic and molecular hopping strength between nearest-neighbor sites. The operators \hat{a}_i and \hat{a}_i^\dagger (\hat{m}_i and \hat{m}_i^\dagger) are bosonic annihilation and creation operators of atoms (molecules) on site i , and operators $\hat{n}_i^a = \hat{a}_i^\dagger \hat{a}_i$ and $\hat{n}_i^m = \hat{m}_i^\dagger \hat{m}_i$ correspond to number operators. Parameter U_a (U_m) is inter-atomic (inter-molecular) on-site interaction, and U_{am} denotes the interaction between atoms and molecules. The chemical potential μ determines the particle filling and g denotes the AMC strength. The parameter Δ corresponds to the so-called detuning that brings the state of two atoms and a molecule in and out of resonance on each site [20,22]. For simplicity, we set parameters $J = J_a = J_m$ and $U = U_a = U_m = U_{am}$ as our numerical calculations. Without loss of generality, we set U as the energy scale.

By using the MF treatment, $\hat{a} = \langle \hat{a} \rangle + \delta$ (same as \hat{m}), and neglecting the second-order fluctuations, the hopping terms are decoupled as

$$\hat{a}_i^\dagger \hat{a}_j \approx \hat{a}_i^\dagger \psi_j^a + \psi_i^{a*} \hat{a}_j - \psi_i^{a*} \psi_j^a \tag{2}$$

and

$$\hat{m}_i^\dagger \hat{m}_j \approx \hat{m}_i^\dagger \psi_j^m + \psi_i^{m*} \hat{m}_j - \psi_i^{m*} \psi_j^m, \tag{3}$$

where $\psi_\sigma^a = \langle \hat{a}_\sigma \rangle$ and $\psi_\sigma^m = \langle \hat{m}_\sigma \rangle$ (here σ denotes i or j) are so-called order parameter. Then the original Hamiltonian (1) is decoupled as

$$\hat{H}_{AMC} = \sum_i \hat{H}_{GMF}^i, \tag{4}$$

with the single-site mean-field Hamiltonian

$$\begin{aligned}
\hat{H}_{GMF}^i = & - 2 \left(J_a \hat{a}_i^\dagger \psi_j^a + J_m \hat{m}_i^\dagger \psi_j^m + H.c. \right) \\
& - 2 \left(J_a |\psi_i^a|^2 + J_m |\psi_i^m|^2 \right) \\
& + \frac{U_a}{2} \hat{n}_i^a (\hat{n}_i^a - 1) + \frac{U_m}{2} \hat{n}_i^m (\hat{n}_i^m - 1) \\
& + U_{am} \hat{n}_i^a \hat{n}_i^m - \mu (\hat{n}_i^a + 2\hat{n}_i^m) \\
& - g \left(\hat{m}_i^\dagger \hat{a}_i \hat{a}_i + \hat{a}_i^\dagger \hat{a}_i^\dagger \hat{m}_i \right) \\
& + \Delta \hat{n}_i^m.
\end{aligned} \tag{5}$$

The Gutzwiller ansatz allows us to express the state of the system as a product of individual single-site states

$$|\Phi_{AMC}\rangle = \prod_i |\phi_{GMF}^i\rangle, \tag{6}$$

where the state of the i th site $|\phi_{GMF}^i\rangle$ can be expanded as

$$|\phi_{GMF}^i\rangle = \sum_{N=0}^{N_{max}} |D_i(N)\rangle, \quad (7)$$

with the dressed Fock state basis

$$|D_i(N)\rangle = \sum_{n^a+2n^m=N} C_{n^a,n^m} |n^a, n^m\rangle. \quad (8)$$

Here, $n^a = \langle D_i(N)|(\hat{n}^a + 2\hat{n}^m)|D_i(N)\rangle$ and $n^m = \langle D_i(N)|(\frac{1}{2}\hat{n}^a + \hat{n}^m)|D_i(N)\rangle$ describe the number of atoms and molecules in the i th site, and $N = n^a + 2n^m$ denotes the total particle number, N_{max} is the truncation of the maximum particle number, and the complex probability amplitudes C_{n^a,n^m} satisfy

$$\sum_{N=0}^{N_{max}} \sum_{n^a+2n^m=N} |C_{n^a,n^m}|^2 = 1.$$

Then the eigenequation $\hat{H}_{AMC}|\Phi_{AMC}\rangle = E|\Phi_{AMC}\rangle$ of the whole system can be simplified as

$$\hat{H}_{GMF}^i|\phi_{GMF}^i\rangle = E_i|\phi_{GMF}^i\rangle, \quad (9)$$

with $E = \sum_i E_i$. The ground state and the order parameter can be obtained from the single-site eigenequation (9) by giving the parameters U , J , g , μ , and Δ . It is worth noting that the MF order parameters of different sites are equal to each other, and then we define $\psi^a = \psi_i^a = \psi_j^a$ and $\psi^m = \psi_i^m = \psi_j^m$.

3. The Effects of AMC and Detuning on Ground-State Phase Diagram

In this section, we will show how the AMC and detuning affect the ground-state phase diagram for the Bose–Hubbard model (1). In Section 3.1, we show the AMC-induced pair-SF and its robustness against atomic hopping. In Section 3.2, we show detuning caused pairing SF-MI transitions.

3.1. AMC-Induced Pair-Superfluid

In order to distinguish different ground-state phases, we calculate the single-atomic order parameter $\psi^a = \langle \hat{a} \rangle$, pair-atomic order parameter $\psi^{aa} = \langle \hat{a}^2 \rangle$, molecular order parameter $\psi^m = \langle \hat{m} \rangle$, and the corresponding filling number $n^a = \langle \hat{n}^a \rangle$ and $n^m = \langle \hat{n}^m \rangle$. Here, our main focus is on the character of the transition between the distinct pair-SF and MI. In order to show the pair-SF phase more clearly, we show the phase diagram of the pair-atomic order parameter ψ^{aa} in Figure 1a, where we only use even-number basis $\{|D_i(0)\rangle, |D_i(2)\rangle, |D_i(4)\rangle, \dots\}$ in our calculation. On the one hand, our results show that the pair-SF phase of nonzero pair-atomic order parameter can take place for the regime of strong inter-site hopping, $J/U \rightarrow \infty$. On the other hand, for strong repulsion, $J/U \rightarrow 0$, there appear several integer atomic MI lobes. The pair-SF phase has also been found in a one-dimensional extensional BH model with two-particle hopping [30–35]. Different from the previous cases, the appearance of pair-SF phase in our system is a direct result of AMC. As $J \gg U$, the atoms and molecules in each site can freely move between the two adjacent sites. However, due to the regime in which AMC allows two atoms to turn into a molecule and vice versa, the total atomic numbers of the corresponding pair-SF phase must be even-integer numbers per site.

To understand the physical mechanism of pair-SF phase, we explore the filling configurations in the Mott state, namely, what is the most energetically favorable filling factor $|n^a, n^m\rangle$ for a given filling number n^a . In Figure 1b,c, we show the distributions of the probability amplitudes $|C_{n^a,n^m}|^2$ of the ground state for SF ($J/U = 0.1$, $\mu/U = 1.5$) and MI ($J/U = 0.01$, $\mu/U = 1.5$) phases. The MI phases as a triple-peaked state ($|0, 4\rangle, |2, 3\rangle$

and $|4, 2\rangle$) in the probability distribution mean that the total atomic numbers per lattice are even-integer numbers ($n^a = 8$) and the residual atom in each lattice can still freely convert to a diatomic molecule due to strong AMC. This filling configuration favors an imbalanced filling pattern $|n^a, n^m\rangle$, and reflects a similar charge–density–wave order in the Mott state [57–59]. In the SF phase, the pairing atoms can move freely between neighboring cells and there appears a pair-atomic SF, as shown in Figure 2c.

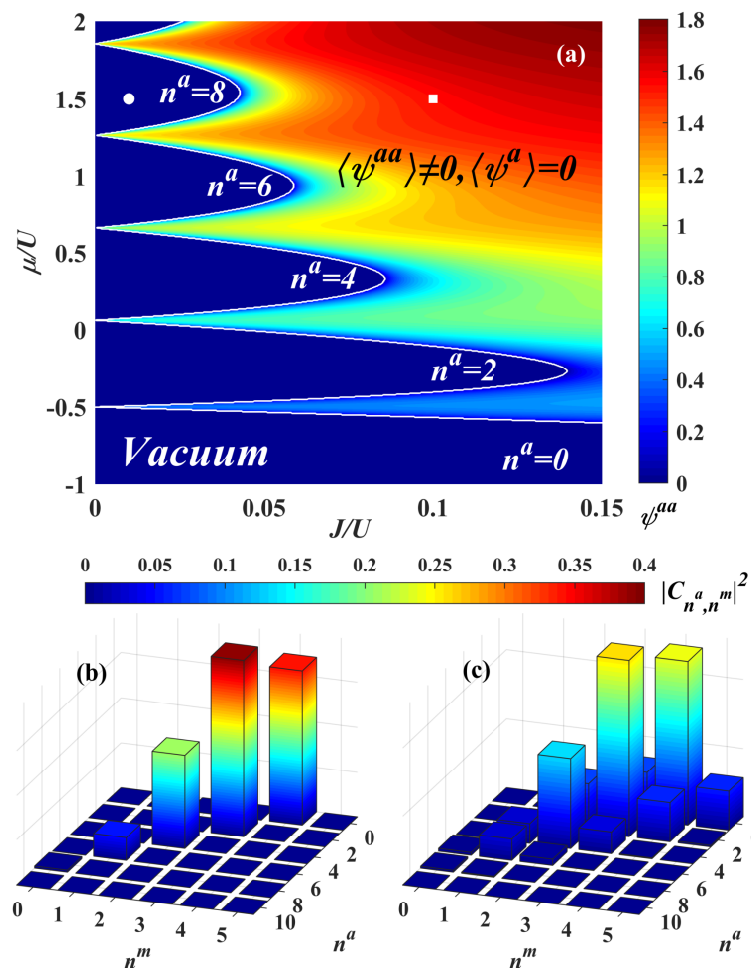


Figure 1. (a) Ground-state phase diagram for the symmetric Bose–Hubbard model ($\Delta = 0$) with AMC, only including even basis. The truncation of maximum particle number N_{max} has been set as $N_{max} = 10$ in our calculation. The blue areas are vacuum and Mott insulator phases with zero and even filling number n^a corresponding to zero-order parameter $\psi^{aa} = 0$, which are surrounded by pair-atomic superfluid phases with nonzero-order parameter $\psi^{aa} \neq 0$. (b,c) The distributions of the probability amplitudes $|C_{n^a, n^m}|^2$ corresponding to the white circle and square in (a), respectively. The other parameters are chosen as $U = 1$ and $g/U = 1$.

Now, we consider the impact of the AMC and hopping strength on the stability of the pair-SF phase. In Figure 2a, we show the ground-state phase diagram in the parameter plane ($J/U, g/U$) for a fixed chemical potential $\mu/U = 1$ by using the full basis $\{|D_i(0)\rangle, |D_i(1)\rangle, |D_i(2)\rangle, \dots\}$ and monitoring both order parameters ψ^a and ψ^{aa} . It is clearly shown that there still exists a pair-SF phase ($\psi^a = 0, \psi^{aa} \neq 0$) in the region of weak AMC strength regardless of the hopping strength. It means that pair-SF induced by the AMC in our system is robust against the hopping. In the strong hopping regime and big AMC strength, $J/U \rightarrow \infty$ and $g/U > 0.5$, and the ground-state is a mixed SF phase consisting of single-atomic and pair-atomic SF ($\psi^a \neq 0, \psi^{aa} \neq 0$). In the strong interaction regime, $J/U \rightarrow 0$, several integer atomic MI lobes ($\psi^a = \psi^{aa} = 0$) appear, where the lobes corre-

sponding to the MI phases with even filling number are greater than the one with odd filling number.

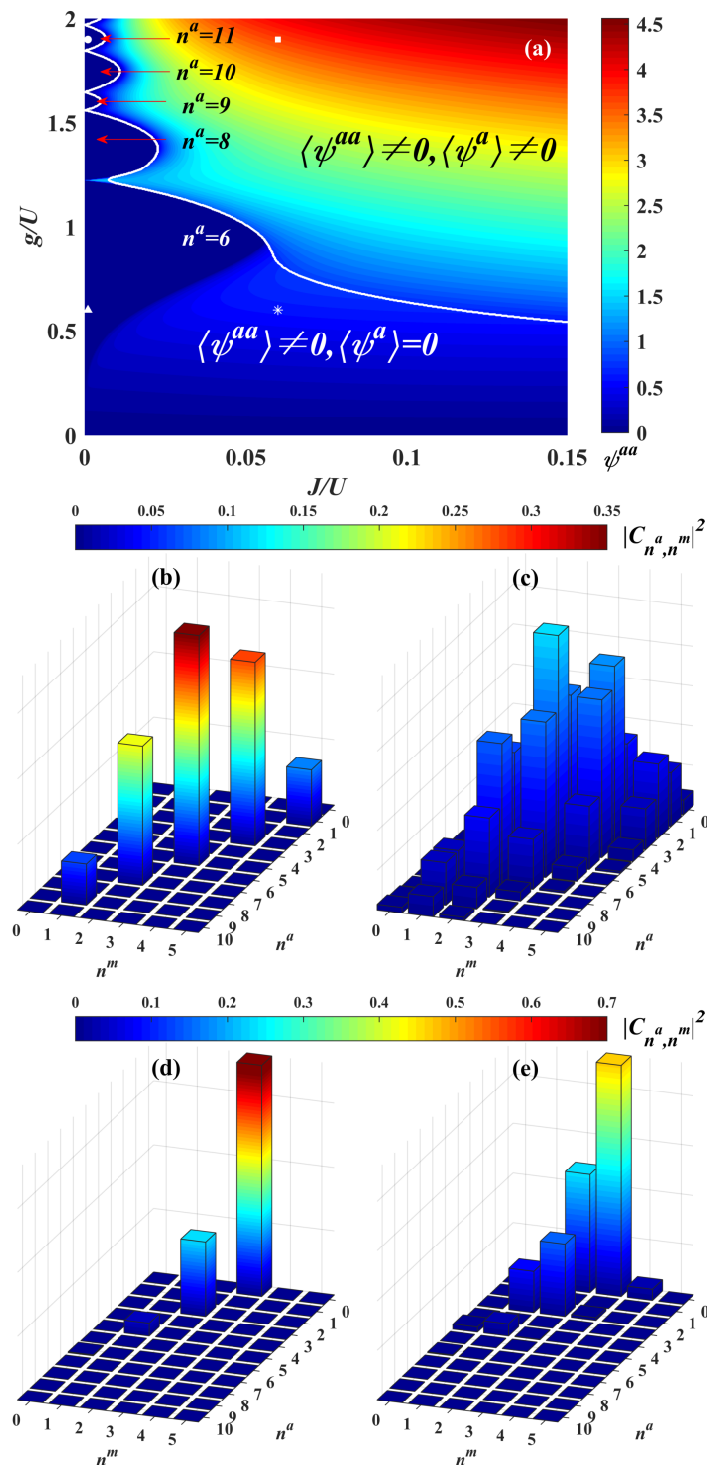


Figure 2. (a) Ground-state phase diagram in the parameter plane $(J/U, g/U)$, including both even and odd basis. The white line indicates the phase boundary of single-atomic SF. As fixing $\mu/U = 1$, the first MI phase has filling number $n_a = 6$. (b,c) The distributions of the probability amplitudes $|C_{n^a, n^m}|^2$ corresponding to the white circle and square in (a), respectively. (d,e) The distributions of the probability amplitudes $|C_{n^a, n^m}|^2$ corresponding to the white triangle and star in (a), respectively. The other parameters are chosen as $\Delta = 0$ and $N_{max} = 10$.

The appearance of the above three phases is a direct result of AMC. In the region of weak AMC, all atoms can adequately convert to a diatomic molecule, and then always generate pair-atomic SF regardless of the hopping strength. However, in the region of strong AMC, all atoms rapidly convert to a diatomic molecule, which may cause the residual single-atomic repulsion, leading to the appearance of single-atomic SF and MI. As $U \gg J$, the tunneling along the chain direction is suppressed and then the order parameter vanishes. However, the atoms in each site may still freely convert to a diatomic molecule due to strong AMC; therefore, the total atomic numbers per site may be even or odd integer numbers. Because the AMC dominates, the insulator phases of even filling numbers are greater than the one with odd filling number.

We also explore the filling configurations of the Mott and superfluid states in three phases. In Figure 2b–e, we show the distributions of the probability amplitudes $|C_{n^a, n^m}|^2$ of the ground state for different SF and MI phases. The MI phase with $n^a = 11$ is also a triple-peaked state ($|3, 4\rangle$, $|5, 3\rangle$ and $|7, 2\rangle$) in the probability distribution, which means that the residual atom in each lattice still freely converts to a diatomic molecule due to strong AMC in the case of the full basis, as shown in Figure 2b. However, the MI phase with $n^a = 6$ is nearly a single-peaked state ($|0, 3\rangle$) in the probability distribution, which means that the residual atom in each lattice cannot freely convert to a diatomic molecule due to weak AMC, as shown in Figure 2c. In the mixed SF phase, the single and pairing atoms can move freely between neighboring cells and there appears a single-atomic and pair-atomic SF along the chain direction, as shown in Figure 2d. In the pair-SF phase, the pairing atoms can only move freely between neighboring cells, though the system deals with the full basis, as shown in Figure 2e.

3.2. Detuning Causes Pair SF-MI Transitions

In this subsection, we show how the detuning Δ affects single-atomic and pair-atomic SF-MI transitions in the strong AMC regime. In Figure 3, we show the ground-state phase diagram of the two order parameters (ψ^a , ψ^{aa}) in the $(\Delta/U, \mu/U)$ plane for $J = 0.01$ and $g = 1$. First, let us consider the single-atomic and pair-atomic Mott states. The Mott states with even n^a are stable on both sides of the detuning; for $\Delta > 0$, there are n^a atoms per site, whereas for $\Delta < 0$, there are $n^m = n^a/2$ molecules per site, due to a negative detuning from Feshbach resonance favoring the formation of molecules [21]. For odd n^a , the MIs are stable only for $\Delta > 0$. For $\Delta < 0$, the ground state with odd n^a is a superposition of two Mott phases with $(n^a - 1)/2$ and $(n^a + 1)/2$ molecules per site and hence unstable to superfluidity for any finite J . Now we will consider the single-atomic and pair-atomic superfluid states. For $\Delta < 0$, it is clear that there are some line-like single-atomic SF phases, and the Mott insulators are sandwiched between different single-atomic SF phases. There appear several parallel and equal-spaced pair-SF stripes. The pair-SF stripes become narrower and their corresponding values become smaller as the chemical potential μ decreases from the positive to the negative side. For a given chemical potential, a sequence of pair SF-MI or MI-SF transitions takes place when the detuning Δ increases from negative to positive. It is important to note that pair-SF phases can split to mixed SF phases consisting of single-atomic and pair-atomic SF ($\psi^a \neq 0$, $\psi^{aa} \neq 0$) after $\Delta > 0$, in which the MI phases with odd n^a are sandwiched. Therefore, the positive detuning Δ can bifurcate AMC-induced pair-SF. Because Δ is related to the energy of a molecular bound state, and a negative detuning favors the formation of molecules, when $\Delta > 0$, the atoms do not like to convert to a diatomic molecule, which may cause the single-atomic hopping and repulsion, leading to the appearance of single-atomic SF and MI. Therefore, the big and positive detuning Δ can bifurcate the pair-SF into mixed SF phases consisting of single-atomic and pair-atomic SF. In addition, the phase transitions of pairing SF-MI or MI-SF in our system, which are driven by the ratio J/U or Δ/U at fixed inter-filling, belong to the class of O(2) transitions. In the following, we will explore how to extract the signature of such phase transitions.

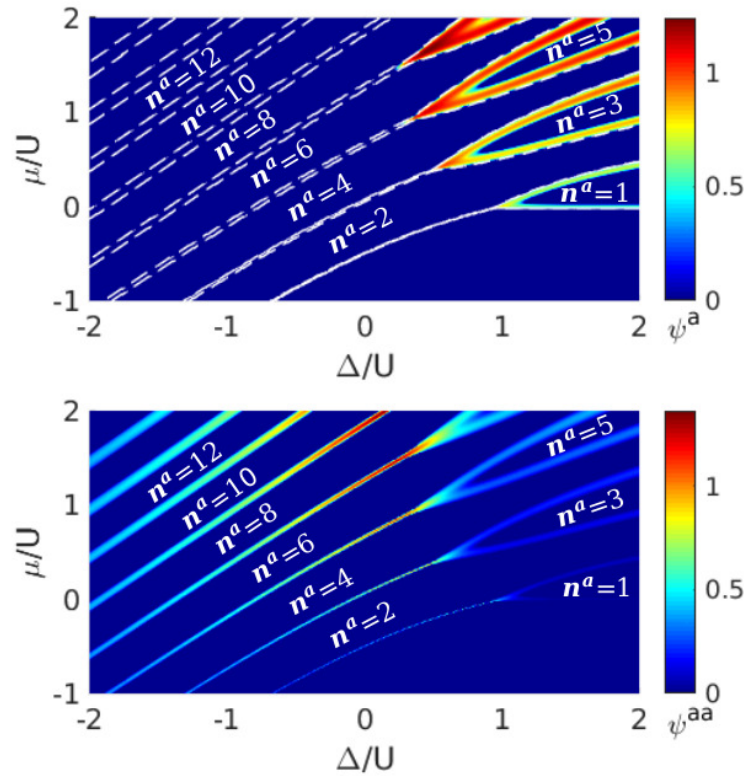


Figure 3. Single-atomic (**Top**) and pair-atomic (**Bottom**) phase diagrams in the parameter plane $(\Delta/U, \mu/U)$. The other parameters are chosen as $g = 1, J = 0.01$, and $U = 1$.

4. The Signature of Phase Transitions

In this analysis, we focus on extracting the signature of the Rényi EE for the pairing SF-MI or MI-SF transitions in our system. The Rényi EE, a well-known bipartite entanglement measure, is defined by dividing the entire system into two subsystems. Since our MF method preserves only the intracell correlations, we only need to consider intracell bipartite entanglement. Denoting the two subsystems as a (atom) and m (molecule), the second-order Rényi EE can be defined as [55,56]

$$S_2(\sigma) = -\log \text{Tr}(\hat{\rho}_\sigma^2), \quad (10)$$

where $\sigma = a, m$, $\hat{\rho}_{a(m)} = \text{Tr}_{m(a)}(\hat{\rho}_{am})$ is the reduced density matrix of subsystem a (m), and $\hat{\rho}_{am}$ is the density matrix of the whole system. From the single-site ground-state, Equation (7), the reduced density matrices $\hat{\rho}_a$ and $\hat{\rho}_m$ are given as

$$\begin{aligned} \hat{\rho}_a &= \sum_{n^a, n^{a'}} \left(\sum_{n^m} C_{n^a, n^m} C_{n^{a'}, n^m}^* \right) |n^a\rangle \langle n^{a'}|, \\ \hat{\rho}_m &= \sum_{n^m, n^{m'}} \left(\sum_{n^a} C_{n^a, n^m} C_{n^a, n^{m'}}^* \right) |n^m\rangle \langle n^{m'}|. \end{aligned} \quad (11)$$

Then the second-order Rényi EE can be calculated by using the above reduced density matrices.

In order to compare, a typical example is displayed in Figure 4a by choosing $\mu/U = 1$ and $\Delta = 0$, which can undergo the phase transition from MI ($\rho(n^a) = 6, \psi_{aa} = 0$) phase to pair-SF ($\psi_{aa} \neq 0$) phase as J/U continuously increase. In Figure 4b, we show the corresponding second-order Rényi EE S_2 (solid blue line) and its first-order derivative $dS_2/d(J/U)$ with respect to J/U (dashed red line). The second-order Rényi EE is continu-

ous everywhere, but a turning point appears at the phase boundary. Indeed, the first-order derivatives (solid red lines) show a drastic jump at the phase boundary. Similarly, the first-order derivative of S_2 with respect to Δ/U also shows drastic jumps at the phase boundaries (see Figure 5). A series of discontinuous peaks that correspond to a sequence of pairing MI-SF or SF-MI transitions appear when the detuning Δ/U increases from negative to positive, and its first-order derivative also shows drastic jumps at the corresponding critical points of phase transitions, as shown in Figure 5. This means that the pairing SF-MI or MI-SF transitions in our system correspond to the jumps in the first-order derivative of the second-order Rényi EE. Therefore, the residual entanglement in our MF treatment can be used to efficiently capture the signature of the pairing SI transition induced by AMC.

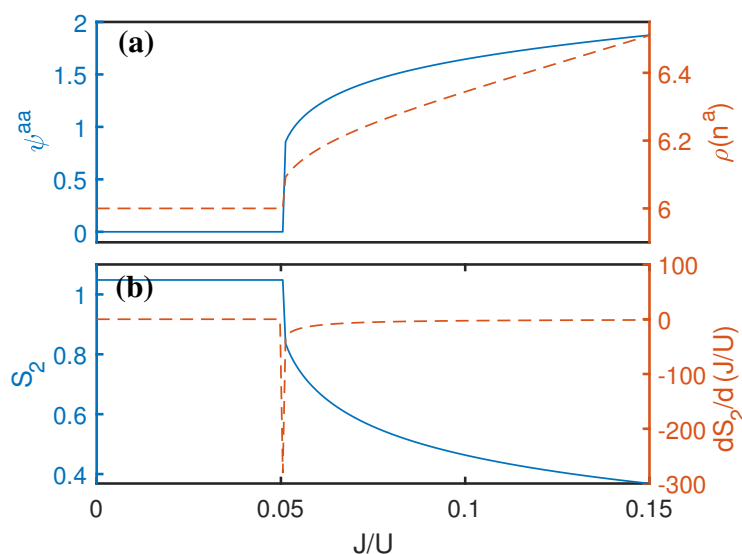


Figure 4. Pair SF-MI transition, second-order Rényi entanglement entropy and its first-order derivative with respect to J/U for $\mu/U = 1$ and $\Delta = 0$. The other parameters are the same as Figure 1. Solid blue and dashed red lines denote ψ^{aa} ($S_2(m)$) and $\rho(n_a)$ ($dS_2/d(J/U)$) in (a,b), respectively.

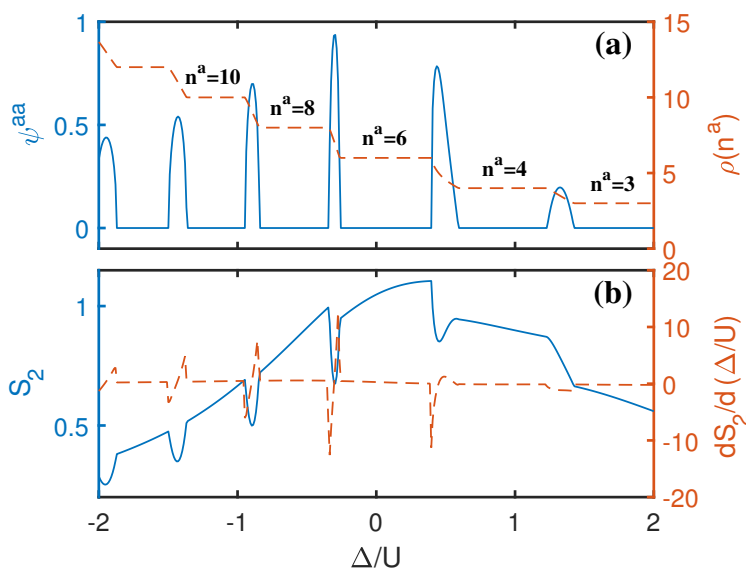


Figure 5. Pair SF-MI transition, second-order Rényi entanglement entropy and its first-order derivative with respect to Δ/U for $\mu/U=1$. The other parameters are the same as Figure 3. Solid blue and dashed red lines denote ψ^{aa} ($S_2(m)$) and $\rho(n_a)$ ($dS_2/d(\Delta/U)$) in (a,b), respectively.

5. Conclusions and Discussion

In summary, we have investigated pairing SI transition and its MF signature of EE for bosonic mixtures of atoms and molecules in one-dimensional optical lattice. In addition to the SF and integer MI phases, we found that AMC can induce an extra pair-SF phase, though the system does not possess a pair-hopping. Depending on the strength of the AMC and the single atomic hopping, the ground state can be an MI, a mixed SF phase with both single-atomic and pair-atomic, or a pair-SF phase. In particular, the ground-state may undergo several pairing SF-MI or MI-SF transitions as the detuning is varied from negative to positive, and the big and positive detuning can bifurcate the pair-SF into mixed SF phases consisting of single-atomic and pair-atomic SF. By calculating the second-order Rényi EE and its first-order derivative, it is revealed that the first-order derivative of the second-order Rényi EE becomes discontinuous at the critical points of the pairing MI-SF or SF-MI transitions. This means that the second-order Rényi EE can be used to extract the signature of the pairing SF-MI phase transition induced by AMC.

The model we propose can be feasibly implemented and its theoretical predictions can be experimentally observed using current techniques. Our proposed bosonic mixtures of atoms and molecules can be demonstrated experimentally in cold-atom setups [11]. By imposing two standing-wave lasers, the one-dimensional optical lattice has been realized [60] and our model can be realized by loading ultracold bosonic mixtures of atoms and molecules in the one-dimensional optical lattice. The strength of AMC g also can be tuned in the experiment via a periodic modulation of the magnetic field [61]. For such a system of bosonic mixtures of atoms and molecules, AMC-induced pairing SI transition may be observed.

Author Contributions: Conceptualization, H.D.; Software, Z.T.; Formal analysis, C.K., F.Y. and H.Z.; Data curation, Z.T. and C.K.; Writing—original draft, H.D.; Supervision, H.Z.; Project administration, H.Z.; Funding acquisition, F.Y. All authors have read and agreed to the published version of the manuscript.

Funding: This work is supported by the National Natural Science Foundation of China under Grant No. 12175315 and No. 12165008.

Data Availability Statement: Data is contained within the article.

Acknowledgments: The authors thank Xiangyuan Chen, Li Zhang and Chaohong Lee for enlightening suggestions and helpful discussions.

Conflicts of Interest: The authors declare no conflict of interest.

References

1. Will, S.; Best, T.; Schneider, U.; Hackermüller, L.; Lxuxhmann, D.-S.; Bloch, I. Time-resolved observation of coherent multi-body interactions in quantum phase revivals. *Nature* **2010**, *465*, 197. [[CrossRef](#)]
2. Soltan-Panahi, P.; Lühmann, D.-S.; Struck, J.; Windpassinger, P.; Sengstock, K. Quantum phase transition to unconventional multi-orbital superfluidity in optical lattices. *Nat. Phys.* **2012**, *8*, 71. [[CrossRef](#)]
3. Bloch, I.; Greiner, M. The superfluid-to-Mott insulator transition and the birth of experimental quantum simulation. *Nat. Rev. Phys.* **2022**, *4*, 739. [[CrossRef](#)]
4. Best, T.; Will, S.; Schneider, U.; Hackermüller, L.; van Oosten, D.; Bloch, I.; Lxuxhmann, D.-S. Role of Interactions in ^{87}Rb - ^{40}K Bose-Fermi Mixtures in a 3D Optical Lattice. *Phys. Rev. Lett.* **2009**, *102*, 030408. [[CrossRef](#)] [[PubMed](#)]
5. Lühmann, D.-S.; Bongs, K.; Sengstock, K.; Pfannkuche, D. Self-Trapping of Bosons and Fermions in Optical Lattices. *Phys. Rev. Lett.* **2008**, *101*, 050402. [[CrossRef](#)]
6. Lutchyn, R.M.; Tewari, S.; Sarma, S.D. Loss of superfluidity by fermions in the boson Hubbard model on an optical lattice. *Phys. Rev. A* **2009**, *79*, 011606. [[CrossRef](#)]
7. Mering, A.; Fleischhauer, M. Multiband and nonlinear hopping corrections to the three-dimensional Bose-Fermi-Hubbard model. *Phys. Rev. A* **2011**, *83*, 063630. [[CrossRef](#)]
8. Jürgensen, O.; Sengstock, K.; Lxuxhmann, D.-S. Density-induced processes in quantum gas mixtures in optical lattices. *Phys. Rev. A* **2012**, *86*, 043623. [[CrossRef](#)]
9. Radzihovsky, L.; Park, J.; Weichman, P.B. Superfluid transitions in bosonic atom-molecule mixtures near a Feshbach resonance. *Phys. Rev. Lett.* **2004**, *92*, 160402. [[CrossRef](#)]

10. Duine, R.A.; Stoof, H.T.C. Atom—Molecule coherence in Bose gases. *Phys. Rep.* **2004**, *396*, 115. [[CrossRef](#)]
11. Zhang, Z.; Chen, L.; Yao, K.-X.; Chin, C. Transition from an atomic to a molecular Bose-Einstein condensate. *Nature* **2021**, *592*, 708. [[CrossRef](#)] [[PubMed](#)]
12. Syassen, N.; Bauer, D.M.; Lettner, M.; Dietze, D.; Volz, T.; Dürr, S.; Rempe, G. Atom-Molecule Rabi Oscillations in a Mott Insulator. *Phys. Rev. Lett.* **2007**, *99*, 033201. [[CrossRef](#)] [[PubMed](#)]
13. Olsen, M.L.; Perreault, J.D.; Cumby, T.D.; Jin, D.S. Coherent atom-molecule oscillations in a Bose-Fermi mixture. *Phys. Rev. A* **2009**, *80*, 030701. [[CrossRef](#)]
14. Abdullaev, F.K.; Ögren, M.; Yuldashev, J.S. Matter waves in atomic-molecular condensates with Feshbach resonance management. *Phys. Rev. E* **2021**, *104*, 024222. [[CrossRef](#)]
15. Romans, M.W.J.; Duine, R.A.; Sachdev, S.; Stoof, H.T.C. Quantum Phase Transition in an Atomic Bose Gas with a Feshbach Resonance. *Phys. Rev. Lett.* **2004**, *93*, 020405. [[CrossRef](#)] [[PubMed](#)]
16. Radzihovsky, L.; Weichman, P.B.; Park, J.I. Superfluidity and phase transitions in a resonant Bose gas. *Ann. Phys.* **2008**, *323*, 2376. [[CrossRef](#)]
17. Ejima, S.; Bhaseen, M.J.; Hohenadler, M.; Essler, F.H.L.; Fehske, H.; Simons, B.D. Ising deconfinement transition between Feshbach-resonant superfluids. *Phys. Rev. Lett.* **2011**, *106*, 015303. [[CrossRef](#)]
18. Bhaseen, M.J.; Ejima, S.; Essler, F.H.L.; Fehske, H.; Hohenadler, M.; Simons, B.D. Discrete symmetry breaking transitions between paired superfluids. *Phys. Rev. A* **2012**, *85*, 033636. [[CrossRef](#)]
19. Dickerscheid, D.B.M.; Khawaja, U.A.; van Oosten, D.; Stoof, H.T.C. Feshbach resonances in an optical lattice. *Phys. Rev. A* **2005**, *71*, 043604. [[CrossRef](#)]
20. Rousseau, V.G.; Denteneer, P.J.H. Quantum phases of mixtures of atoms and molecules on optical lattices. *Phys. Rev. A* **2008**, *77*, 013609. [[CrossRef](#)]
21. VRousseau, G.; Denteneer, P.J.H. Feshbach-Einstein Condensates. *Phys. Rev. Lett.* **2009**, *102*, 015301. [[CrossRef](#)] [[PubMed](#)]
22. Parny, L.D.D.; Rousseau, V.G.; Roscilde, T. Feshbach-Stabilized Insulator of Bosons in Optical Lattices. *Phys. Rev. Lett.* **2015**, *114*, 195302. [[CrossRef](#)]
23. Sengupta, K.; Dupuis, N. Mott insulator to superfluid transition of ultracold bosons in an optical lattice near a Feshbach resonance. *Europhys. Lett.* **2005**, *70*, 586. [[CrossRef](#)]
24. Timmermans, E.; Tommasini, P.; Hussein, M.; Kerman, A. Feshbach resonances in atomic Bose-Einstein condensates. *Phys. Rep.* **1999**, *315*, 199. [[CrossRef](#)]
25. Kóler, T.; Gxoxal, K. Production of cold molecules via magnetically tunable Feshbach resonances. *Rev. Mod. Phys.* **2006**, *78*, 1311. [[CrossRef](#)]
26. Chin, C.; Grimm, R.; Julienne, P.; Tiesinga, E. Feshbach resonances in ultracold gases. *Rev. Mod. Phys.* **2010**, *82*, 1225. [[CrossRef](#)]
27. Rousseau, V.G.; Hettiarachchilage, K.; Jarrell, M.; Moreno, J.; Sheehy, D.E. Using off-diagonal confinement as a cooling method. *Phys. Rev. A* **2010**, *82*, 063631. [[CrossRef](#)]
28. Sun, J.; Zhao, P.; Hu, Z.; Jin, S.; Liao, R.; Liu, X.-J.; Chen, X. Observation of 2D Mott insulator and π -superfluid quantum phase transition in shaking optical lattice. *arXiv* **2023**, arXiv:2306.04477.
29. Hettiarachchilage, K.; Rousseau, V.G.; Tam, K.-M.; Jarrell, M.; Moreno, J. Phase diagram of the Bose-Hubbard model on a ring-shaped lattice with tunable weak links. *Phys. Rev. A* **2013**, *87*, 051607. [[CrossRef](#)]
30. Zhou, X.F.; Zhang, Y.S.; Guo, G.C. Pair tunneling of bosonic atoms in an optical lattice. *Phys. Rev. A* **2009**, *80*, 013605. [[CrossRef](#)]
31. Schmidt, K.P.; Dorier, J.; Läuchli, A.; Mila, F. Single-particle versus pair condensation of hard-core bosons with correlated hopping. *Phys. Rev. B* **2006**, *74*, 174508. [[CrossRef](#)]
32. Bonnes, L.; Wessel, S. Pair superfluidity of three-body constrained bosons in two dimensions. *Phys. Rev. Lett.* **2011**, *106*, 185302. [[CrossRef](#)] [[PubMed](#)]
33. Mazza, L.; Rizzi, M.; Lewenstein, M.; Cirac, J.I. Emerging bosons with three-body interactions from spin-1 atoms in optical lattices. *Phys. Rev. A* **2010**, *82*, 043629. [[CrossRef](#)]
34. Eckholt, M.; García-Ripoll, J.J. Pair condensation of bosonic atoms induced by optical lattices. *Phys. Rev. A* **2008**, *77*, 063603. [[CrossRef](#)]
35. Lebreuilly, J.; Aron, C.; Mora, C. Stabilizing Arrays of Photonic Cat States via Spontaneous Symmetry Breaking. *Phys. Rev. Lett.* **2019**, *122*, 120402. [[CrossRef](#)]
36. Hu, A.; Mathey, L.; Williams, C.J.; Clark, C.W. Noise correlations of one-dimensional Bose mixtures in optical lattices. *Phys. Rev. A* **2010**, *81*, 063602. [[CrossRef](#)]
37. Grémaud, B.; Batrouni, G.G. Pairing and Pair Superfluid Density in One-Dimensional Two-Species Fermionic and Bosonic Hubbard Models. *Phys. Rev. Lett.* **2021**, *127*, 025301. [[CrossRef](#)]
38. Sellin, K.; Babaev, E. Superfluid drag in the two-component Bose-Hubbard model. *Phys. Rev. B* **2018**, *97*, 094517. [[CrossRef](#)]
39. Hu, A.; Mathey, L.; Danshita, I.; Tiesinga, E.; Williams, C.J.; Clark, A.C.W. Counterflow and paired superfluidity in one-dimensional Bose mixtures in optical lattices. *Phys. Rev. A* **2009**, *80*, 023619. [[CrossRef](#)]
40. Hu, A.; Mathey, L.; Tiesinga, E.; Danshita, I.; Williams, C.J.; Clark, A.C.W. Detecting paired and counterflow superfluidity via dipole oscillations. *Phys. Rev. A* **2011**, *84*, 041609. [[CrossRef](#)]
41. Osborne, T.J.; Nielsen, M.A. Entanglement in a simple quantum phase transition. *Phys. Rev. A* **2002**, *66*, 032110. [[CrossRef](#)]

42. Vidal, G.; Latorre, J.I.; Rico, E.; Kitaev, A. Entanglement in Quantum Critical Phenomena. *Phys. Rev. Lett.* **2003**, *90*, 227902. [[CrossRef](#)] [[PubMed](#)]
43. Latorre, J.I.; Rico, E.; Vidal, G. Ground state entanglement in quantum spin chains. *Quantum Inf. Comput.* **2004**, *4*, 48.
44. Carrasco, J.A.; Finkel, F.; González-López, A.; Rodríguez, M.A.; Tempesta, P. Generalized isotropic Lipkin-Meshkov-Glick models: Ground state entanglement and quantum entropies. *J. Stat. Mech.* **2016**, *2016*, 033114. [[CrossRef](#)]
45. Gu, S.-J.; Deng, S.-S.; Li, Y.-Q.; Lin, H.-Q. Entanglement and Quantum Phase Transition in the Extended Hubbard Model. *Phys. Rev. Lett.* **2004**, *93*, 086402. [[CrossRef](#)]
46. Anfossi, A.; Giorda, P.; Montorsi, A.; Traversa, F. Two- Point Versus Multipartite Entanglement in Quantum Phase Transitions. *Phys. Rev. Lett.* **2005**, *95*, 056402. [[CrossRef](#)]
47. Anfossi, A.; Boschi, C.D.E.; Montorsi, A.; Ortolani, F. Single-site entanglement at the superconductor-insulator transition in the Hirsch model. *Phys. Rev. B* **2006**, *73*, 085113. [[CrossRef](#)]
48. You, W.-L. The scaling of entanglement entropy in a honeycomb lattice on a torus. *J. Phys. A* **2014**, *47*, 255301. [[CrossRef](#)]
49. Buonsante, P.; Vezzani, A. Ground-State Fidelity and Bipartite Entanglement in the Bose-Hubbard Model. *Phys. Rev. Lett.* **2007**, *98*, 110601. [[CrossRef](#)]
50. Läuchli, A.M.; Kollath, C. Spreading of correlations and entanglement after a quench in the one-dimensional Bose-Hubbard model. *J. Stat. Mech.* **2008**, *2008*, P05018. [[CrossRef](#)]
51. Silva-Valencia, J.; Souza, A.M.C. First Mott lobe of bosons with local two- and three-body interactions. *Phys. Rev. A* **2011**, *84*, 065601. [[CrossRef](#)]
52. Pino, M.; Prior, J.; Somoza, A.M.; Jaksch, D.; Clark, S.R. Reentrance and entanglement in the one-dimensional Bose-Hubbard model. *Phys. Rev. A* **2012**, *86*, 023631. [[CrossRef](#)]
53. Alba, V.; Haque, M.; Läuchli, A.M. Entanglement Spectrum of the Two-Dimensional Bose-Hubbard Model. *Phys. Rev. Lett.* **2013**, *110*, 260403. [[CrossRef](#)] [[PubMed](#)]
54. Frérot, I.; Roscilde, T. Entanglement Entropy Across the Superfluid-Insulator Transition: A Signature of Bosonic Criticality. *Phys. Rev. Lett.* **2016**, *116*, 190401. [[CrossRef](#)]
55. Zhang, L.; Qin, X.; Ke, Y.; Lee, C. Cluster mean-field signature of entanglement entropy in bosonic superfluid-insulator transitions. *Phys. Rev. A* **2016**, *94*, 023634. [[CrossRef](#)]
56. Islam, R.; Ma, R.; Preiss, P.M.; Tai, M.E.; Lukin, A.; Rispoli, M.; Greiner, M. Measuring entanglement entropy in a quantum many-body system. *Nature* **2015**, *528*, 77. [[CrossRef](#)]
57. Chen, B.L.; Kou, S.P.; Zhang, Y.; Chen, S. Quantum phases of the Bose-Hubbard model in optical superlattices. *Phys. Rev. A* **2010**, *81*, 053608. [[CrossRef](#)]
58. Rousseau, V.G.; Arovas, D.P.; Rigol, M.; Hebert, F.; Batrouni, G.G.; Scalettar, R.T. Exact study of the one-dimensional boson Hubbard model with a superlattice potential. *Phys. Rev. B* **2006**, *73*, 174516. [[CrossRef](#)]
59. Batrouni, G.G.; Hébert, F.; Scalettar, R.T. Supersolid Phases in the One-Dimensional Extended Soft-Core Bosonic Hubbard Model. *Phys. Rev. Lett.* **2006**, *97*, 087209. [[CrossRef](#)]
60. Bloch, I.; Dalibard, J.; Zwirger, W. Many-body physics with ultracold gases. *Rev. Mod. Phys.* **2008**, *80*, 885. [[CrossRef](#)]
61. Thompson, S.T.; Hodby, E.; Wieman, C.E. Ultracold Molecule Production via a Resonant Oscillating Magnetic Field. *Phys. Rev. Lett.* **2005**, *95*, 190404. [[CrossRef](#)] [[PubMed](#)]

Disclaimer/Publisher's Note: The statements, opinions and data contained in all publications are solely those of the individual author(s) and contributor(s) and not of MDPI and/or the editor(s). MDPI and/or the editor(s) disclaim responsibility for any injury to people or property resulting from any ideas, methods, instructions or products referred to in the content.